Biosensors and Bioelectronics 85 (2016) 331–336

Contents lists available at ScienceDirect

Biosensors and Bioelectronics

journal homepage: www.elsevier.com/locate/bios

多壁纳米管 MWCNTs based high sensitive lateral flow strip biosensor for rapid determination of aqueous mercury ions

Li Yao [a], Jun Teng [a], Mengya Zhu [a], Lei Zheng [a], Youhao Zhong [a], Guodong Liu [b], Feng Xue [c,*], Wei Chen [a,*]

[a] School of Biotechnology and Food Engineering, Anhui Provincial Key Lab of Functional Materials and Devices, Hefei University of Technology, Hefei 230009, China
[b] Department of Chemistry and Biochemistry, North Dakota State University, Fargo, ND 58105, United States
[c] Jiangsu Entry-Exit Inspection and Quarantine Bureau, Nanjing 200002, PR China

ARTICLE INFO

Article history:
Received 19 March 2016
Received in revised form
28 April 2016
Accepted 8 May 2016
Available online 10 May 2016

Keywords:
Hg^{2+} detection
Carbon nanotube
Lateral flow strip
Sensitivity enhancement
Stability improvement

ABSTRACT

Here, we describe a disposable multi-walled carbon nanotubes (MWCNTs) labeled nucleic acid lateral flow strip biosensor for rapid and sensitive detection of aqueous mercury ions (Hg^{2+}). Unlike the conventional colloidal gold nanoparticle based strip biosensors, the carboxylated MWCNTs were selected as the labeling substrate because of its high specific surface area for immobilization of recognition probes, improved stability and enhanced detection sensitivity of the strip biosensor. Combining the sandwich-type of T-Hg^{2+}-T recognition mechanism with the optical properties of MWCNTs on lateral flow strip, optical black bands were observed on the lateral flow strips. Parameters (such as membrane category, the MWCNTs concentration, the amount of MWCNT-DNA probe, and the volume of the test probe) that govern the sensitivity and reproducibility of the sensor were optimized. The response of the optimized biosensor was highly linear over the range of 0.05–1 ppb target Hg^{2+}, and the detection threshold was estimated at 0.05 ppb within a 15-min assay time. The sensitivity was 10-fold higher than the conventional colloidal gold based strip biosensor. More importantly, the stability of the sensor was also greatly improved with the usage of MWCNTs as the labeling.

1. Introduction

Mercury ion (Hg^{2+}) is a well-known toxic contaminant among most of the heavy metals (Anjaneyulu and Rao, 2001). Considering the detrimental effects of Hg^{2+} on humans (Storelli, 2008), animals (Abdolmohammad-Zadeh and Rahimpour, 2015), and plants (Jun et al., 2016), numerous detection methods have been extensively developed. These traditional methods highly relied on instruments like Ultraviolet Spectrophotometry (Andruch et al., 2012), Atomic Emission Spectrometry (AES) (Chai et al., 2010), Inductively Coupled Plasma Mass Spectrometry (ICP-MS) (Zhang et al., 2016a), HPLC etc. Although these methods have satisfactory detection sensitivity, time-consuming protocols and affluent maintenance limit their usage for on-site detections. In order to suffice these requirements, many rapid detection methods have also been established, mainly including immunoassay (Wang et al., 2014b), gold nanoparticles based colorimetric methods (Chen et al., 2015; Deng et al., 2015; Kalluri et al., 2009), electrochemical methods (Hezard et al., 2013; Zhang et al., 2016b), and Surface enhanced Raman spectroscopy (SERS) (Han et al., 2010; Senapati et al., 2011). Also, the chromatographic lateral flow strip (LFS) method is widely used (Zhu et al., 2014). Colloidal gold nanoparticle (AuNPs) is the usual labeling for the classic LFS (Guo et al., 2012; Mei et al., 2012), because of its easy preparation, excellent biocompatibility (Dhamecha et al., 2016), and the ability to combine with a variety of biological molecules (Liu et al., 2015b). Meanwhile, depending on the classic and specific T-Hg^{2+}-T structure (Liu and Lu, 2007; Tanaka et al., 2006; Xiao et al., 2012), gold nanoparticles would be captured on the nitrocellulose membrane, showing the specific wine red color for results judgements.

However, except for its favorable biocompatibility, the advanced technology to assemble protein or nucleic acid probes onto the surface of AuNPs is not stable at specific conditions because of the instability of the AuNPs under conditions of high concentrations of salt. This requires AuNPs with high quality, which limits the detection sensitivity to a certain extent. Moreover, the assembled AuNPs-based LFS requires specific low temperature, approximately, 4 °C storage conditions. Considering these situations,

* Corresponding authors.
E-mail addresses: xuef1@jsciq.gov.cn (F. Xue), chenweishnu@163.com (W. Chen).

http://dx.doi.org/10.1016/j.bios.2016.05.031
0956-5663/

a great many novel materials have been explored for chromatographic LFS. So far, novel materials like the magnetic nanoparticles (Ge et al., 2013), latex (Mao et al., 2013), and fluorescent materials like quantum dot (Li et al., 2014; Wang et al., 2011) and fluorescent microspheres (Liu et al., 2015a; Wang et al., 2014c; Zhou et al., 2014) are known to be adopted as labeling for LFS. Usage of the rhodamine derivative in a chromatographic test strip, exhibits the excellent selectivity and high sensitivity to Hg^{2+} detection in the aqueous solution (Wang et al., 2014a). Magnetic Fe_3O_4@TiO_2 nanoparticles have also been applied in detecting phosphorylated butyryl cholinesterase with exciting findings (Ge et al., 2013).

In this article, we adopt carbon nanotubes (CNTs) as the chromogenic labeling substrate. CNTs were first discovered in 1991 by Sumio Iijima in NEC Research Institute (Burstein, 2003). They are divided into multi-walled and single-walled carbon nanotubes. Because of their unique structure and peculiar physical, chemical and mechanical properties rendering potentially robust applications (Du et al., 2015), they have attracted much attention from various research fields (Sanchez-Valencia et al., 2014). CNTs have similar lamellar structure as graphite and its structural and geometric characteristics determine the unique electrical properties (Li et al., 2004). In addition, the mechanical properties of CNTs have also become a popular subject for nanotechnology and analytical research (Luo et al., 2008). Theoretical calculations show that CNTs have high strength and excellent toughness, but most of all, they have larger surface area (Wu et al., 2009). There are numerous pores in their special pipeline structure and between the core portions that leads to the large specific surface area. Due to these characteristics, a mass of bioactive molecules can be assembled on the surface, resulting in the application of CNTs in biological detection technology (He et al., 2005; Holder and Francis, 2007; Li et al., 2005).

Although CNTs also have a potential for sensor applications, there are only a few reports of CNT-labeled LFS biosensor for online biochemical detection of the aqueous environmental samples (Liao et al., 2015; Martínez et al., 2012). Furthermore, since CNTs aggregate easily, they are almost insoluble in any organic solvent, and have very weak invasive ability on other types of molecules. Thus, CNTs cannot be a solution or a uniform dispersion of the composite material which severely limits their application in various fields (Gojny et al., 2003; Lou et al., 2004; Pirlot et al., 2003; Ramanathan et al., 2005). In order to expand their usages, the CNTs should be functionalized in advance based on the covalent and non-covalent reaction mechanisms (Giovanni et al., 2010). Covalent functionalization is the treating of the CNTs with a mixed acid or other strong oxidant, connecting the carboxyl, hydroxyl, amino and other reactive groups to their sidewall or port in the form of covalent bonds (Panchakarla and Govindaraj, 2008). In this research, the commercial multi-walled carbon nanotubes (MWCNTs) were functionalized with carboxyl groups followed by the combination of the aminated oligonucleotide recognition probes. Furthermore, in the presence of mercury ions (Hg^{2+}), MWCNTs could be captured on the test line of the LFS sensor owing to the interaction between the nucleic acid probes and Hg^{2+}. Ascribing to the larger surface area of MWCNTs, this MWCNT-labeled LFS method has higher detection sensitivity compared to traditional AuNPs-based LFS. And, more importantly, the stability of the MWCNT-labeled LFS is also greatly improved due to the covalent conjugation of recognition probes onto the functionalized MWCNTs.

2. Experimental

2.1. Materials and reagents

Carboxylated multi-walled carbon nanotubes (MWCNT) with the length of 0.5–2 μm and out diameter < 8 nm were purchased from Nanjing Xian-Feng Nanomaterials Technology Co., Ltd. Streptavidin (SA), carbodiimide hydrochloride (EDC), N-Hydroxysuccinimide (NHS), and bovine serum albumin (BSA) were purchased from Sangon Biotechnical Engineering Co., Ltd. Other chemicals such as sodium chloride (NaCl), potassium chloride (KCl), magnesium chloride ($MgCl_2$), trisodium phosphate (Na_3PO_4), sucrose, trehalose, polyethylene glycol (PEG), cetyltrimethyl ammonium bromide (CTAB), hydrochloric acid (HCl), Tween-20, Triton X-100, sodium dodecyl sulfate (SDS), Tris(hydroxymethyl) aminomethane were purchased from Sinopharm Chemical Reagent Co., Ltd. All the reagents were of analytical grade and solutions were prepared with ultrapure water. The DNA oligonucleotide sequences were as follows:

Test probe1: 5′-NH2-ACA CGC CAT CAA GCT TTA ACT CAT AGT GGC GTG TCG CG-3′; Test probe2: 5′-SH–ACA CGC CAT CAA GCT TTA ACT CAT AGT GGC GTG TCG CG-3′; T line probe: 5′-Biotin-TTC GCT CTC TTT GTG TTT TTG CAT GT-3′; C line probe: 5′-Biotin-ACG CGA CAC GCC ACT ATG AG-3′.

2.2. Conjugation of MWCNTs with test probes (MWCNT-DNA)

The MWCNT-DNA was prepared as follows: 70 μL of 2 μM aminated DNA oligonucleotide test probe 1 was activated with 120 μL 40 mM EDC and 80 μL 40 mM NHS in a clean glass bottle with shaking for 3 h in dark at room temperature (RT). Subsequently, 200 μL of 5 mg/mL MWCNT solution was added followed by 12 h incubation. The mixture was centrifuged at 8500*g* for 6 min to discard the excess reagent and the precipitate was resuspended in the buffer (1 mM Tris–HCl containing 5% BSA, 0.25% Tween-20, 10% sucrose). Finally, each conjugate pad of LFS was sprayed with the 8.5 μL MWCNT-DNA conjugates and dried at 37 °C for further use.

2.3. Preparation of composite probes for control line (C-line) and test line (T-line) of LFS

The composite probes for control line were prepared as follows: 20 μL 100 μM C-line probe and 14 μL 83.3 μM streptavidin were mixed in clean glass bottle and incubated for 3 h at RT, following to which 66 μL 1 mM PBS (pH 7.4) was added to the mixture. The reaction was mixed thoroughly for further use. The composite probes for T-line were essentially prepared in the same way by substituting the C-line probe with the T-line probe. The two composite probes are sprayed on the nitrocellulose membrane respectively to form two parallel T- and C-line on the membrane.

2.4. Preparation of MWCNT-LFS biosensor

The LFS was made up of plastic plate, sample pad, conjugate pad, nitrocellulose membrane, and absorbent pad. Before assembling together, the sample pad and conjugation pad are specifically treated. Firstly, the two pads are socked in the sample pad treating solution (0.05 M Tris–HCl pH 8.0, 0.25% Triton X-100, 0.15 mM NaCl) followed by conjugation pad treating solution (0.01 M PBS pH 7.4, 5% sucrose, 0.3% Tween-20) for 2 h, and then baked in the oven. The five parts are then assembled together to form a complete chromatographic MWCNT-labeled LFS biosensor.

3. Results and discussions

Fig. 1 The MWCNT-labeled LFS biosensor for Hg^{2+} detection is schematically depicted in Fig. 1. The functionalized MWCNTs are covalently conjugated with the test probe and the composite probes are sprayed onto the conjugation pad of LFS. In the presence of the target Hg^{2+}, the MWCNTs labeled test probes are captured and retained on the test line of the strip with the formation of the specific T-Hg^{2+}-T structure. The accumulation of the retained MWCNTs on the test line induces the occurrence of the distinguished black signal on the test line. Due to the stability of the MWCNT-DNA conjugates, the sensitivity and the stability of the traditional LFS are both improved greatly.

3.1. The optimization of experimental parameters

Fig. 2 The nitrocellulose (NC) membrane from different manufacturers and of different models had different pore size and chromatographic performance, which directly affected the sensitivity, coloration intensity and noise signal. Considering this scenario, four types of NC membranes including Millipore 135 (a), Vivid 170 (b), CN 140 (c), Pall 170 (d) were chosen to optimize the most appropriate type in our research (Fig. 2(A)). All four strips were tested with the sample containing 1 ppb Hg^{2+}. The outcome displayed in Fig. 2(A), wherein both of the C- and T-lines were blurred in Vivid 170 (b), the sensitivity of the CN140 strip was too low (c), while that of the T-line of Pall 170 was intermittent (d). On the whole, the sensitivity of Millipore 135 was comparatively satisfied. The main reason of low sensitivity was due to the extremely small pore size of Vivid 170 and CN 140 membranes that affected the tomographic capability of the MWCNTs, leading to less MWCNTs flow though the membrane and blurred lines on the strips. On the other hand, ascribing to the unstable hydrophilic property, the chromatographic progress of the sample solution is inhomogeneous, causing the intermittent lines.

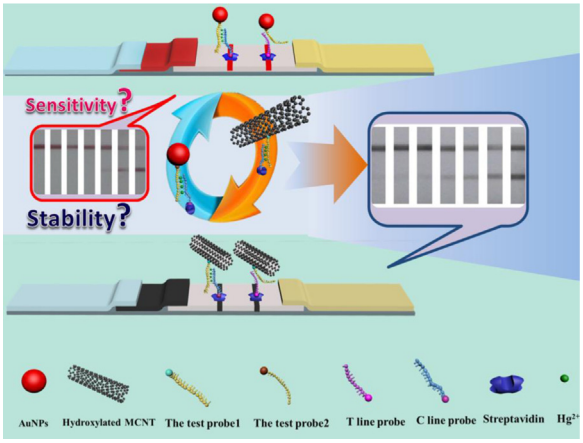

Fig. 1. The schematic diagram of the MWCNTs labeled lateral flow strip biosensor for mercury ion detection.

The MWCNTs, acting as the signal reporting tags in this method, directly affected the detection sensitivity. Hence, the concentration should be carefully optimized in order to achieve the superlative sensitivity. When MWCNTs concentration was higher than the optimal concentration, it caused the background interference impeding detection. Lower than the optimal, resulted in a very weak intensity of the test line for determination. Only the optimal MWCNTs concentration resulted in both an intense line and the best signal-to-noise (S/N) results. Four different concentrations (1 mg/mL, 2 mg/mL, 5 mg/mL and 10 mg/mL) of MWCNTs were interrogated as the optimized concentration parameters on the conjugation pad for measuring samples with 1 ppb Hg^{2+} (Fig. 2B and Fig. S1 in SI). Together, these results indicated that the signal of test line was directly proportional to increased MWCNTs concentration, and reached a maximum at 10 mg/mL (d), while it was weakest at 1 mg/mL concentration (a) along with weak line intensity. Although the background interference of 2 mg/mL (b) was at the same level of 5 mg/mL (c), the later (5 mg/mL) deems to be the most suitable concentration for subsequent research considering the S/N results.

Furthermore, to investigate the effect of the volume of the recognition probe on the sensitivity, different volumes (30 μL, 50 μL, 70 μL, and 100 μL) of the test probe 1 were covalently combined with 200 μL of MWCNTs solution, respectively. According to the results in Fig. 1C and supporting information, the intensity of the black bands on the test and control zone increases gradually from 30 to 100 μL. However, the intensity of the black band did not increase significantly when the volume of the test probe was

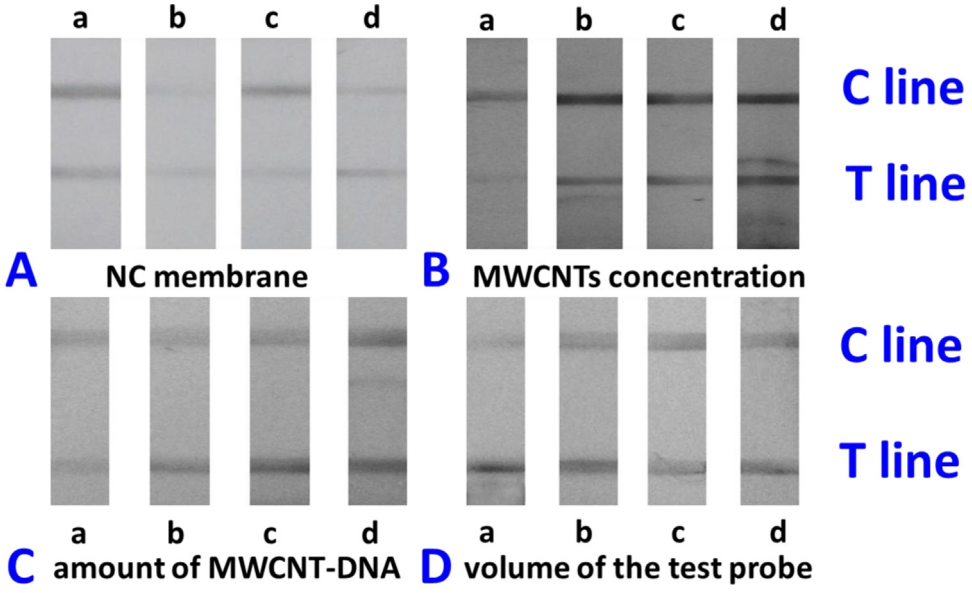

Fig. 2. Optimization results of the experimental parameters of MWCNT-LFS biosensor (A) NC membrane optimization; (B) concentration of MWCNTs for labeling; (C) the amount of MWCNT-DNA probes on conjugation pad of LFS; (D) the volume of the test probe on T-line of the LFS.

increased up to 100 μL or higher (Fig. S2). Hence, 100 μL was selected as the final volume of the test probe.

In the present study, MWCNT-DNA was used as a recognition probe for the detection of Hg^{2+}, and the accumulation of MWCNT-DNA in the test and control lines is visualized as the characteristic black band, which could be adopted for qualitative and quantitative analysis of the target Hg^{2+}. Nevertheless, the amount of MWCNT-DNA composites on the conjugation pad is a significant factor directly affecting the sensitivity, which was controlled from 3 to 10 μL for the optimization. Fig. 1(D) represents the recorded intensity of the lines for 1 ppb of target Hg^{2+} tested with the different amounts of MWCNT-DNA composites loaded conjugation pads. The test line intensity is almost consistent when the volume is 3 or 5 μL, but decreased when the volume is increased to 7 μL or higher. This could be mainly because excess MWCNT-DNA on the conjugation pad blocks the pores and hinders the release of the composites on the NC membrane, resulting in a lower sensitivity. Concurrently, 5 μL MWCNT-DNA composite exhibits maximum intensity for the control line, and hence, this volume was used for all the following research. Another important factor of the sensing is the recognition time between the T-rich probes and target Hg^{2+}. Based on the previous reports, the recognition reaction between the T-rich probe and target Hg^{2+} could be completed in less than 2 min (Li et al., 2008; Liu et al., 2007) and the reaction time of the lateral flow strip based methods usually takes no more than 15 min (Mei et al. 2013; Zhu et al. 2014), the recognition of the target Hg^{2+} could be thoroughly guaranteed on the platform of the lateral flow strip.

3.2. Detection of Hg^{2+} under optimal experimental conditions

Fig. 3 To evaluate the sensitivity and dynamic range of the MWCNT-LFS biosensor for Hg^{2+} detection, we examined the performance of the test strip at different concentrations of target Hg^{2+} prepared in the running buffer (10 mM Tris–HCl, 5 mM $MgCl_2$, 5 mM KCl, 1% BSA, 4 × SSC, 1% Tween-20, 1 mM CTAB, 2% PEG). As shown in Fig. 3(A), the optical intensity of the black bands on the test zone increased with increasing amount of Hg^{2+} in the samples. In the absence of Hg^{2+}, there was no band observed on the test zone. The corresponding optical densities were further confirmed by recording the optical density values of the black bands on the test zone with ImageJ (Fig. 3(B)). The resulting calibration curve showed that the gray value was proportional to the amount of Hg^{2+} in the range from 0.01 to 5 ppb (inset image in Fig. 3(C)) and good linear relationship was achieved in the range from 0.05 to 1 ppb with a correlation coefficient of 0.991 (Fig. 3 (C)). The black band on the test zone was visible even at 0.05 ppb, which could be marked as the threshold for the visual determination of Hg^{2+}, without instrumentation, in a standard sample.

3.3. Comparison the MWCNT-labeled strip biosensor with traditional colloidal gold labeled biosensor

The traditional LFS method is based on colloidal gold nanoparticle as the labeling substrate, and the fundamental purpose of the current study was to increase the detection sensitivity and stability in case of the replacement of the labeling substrate.

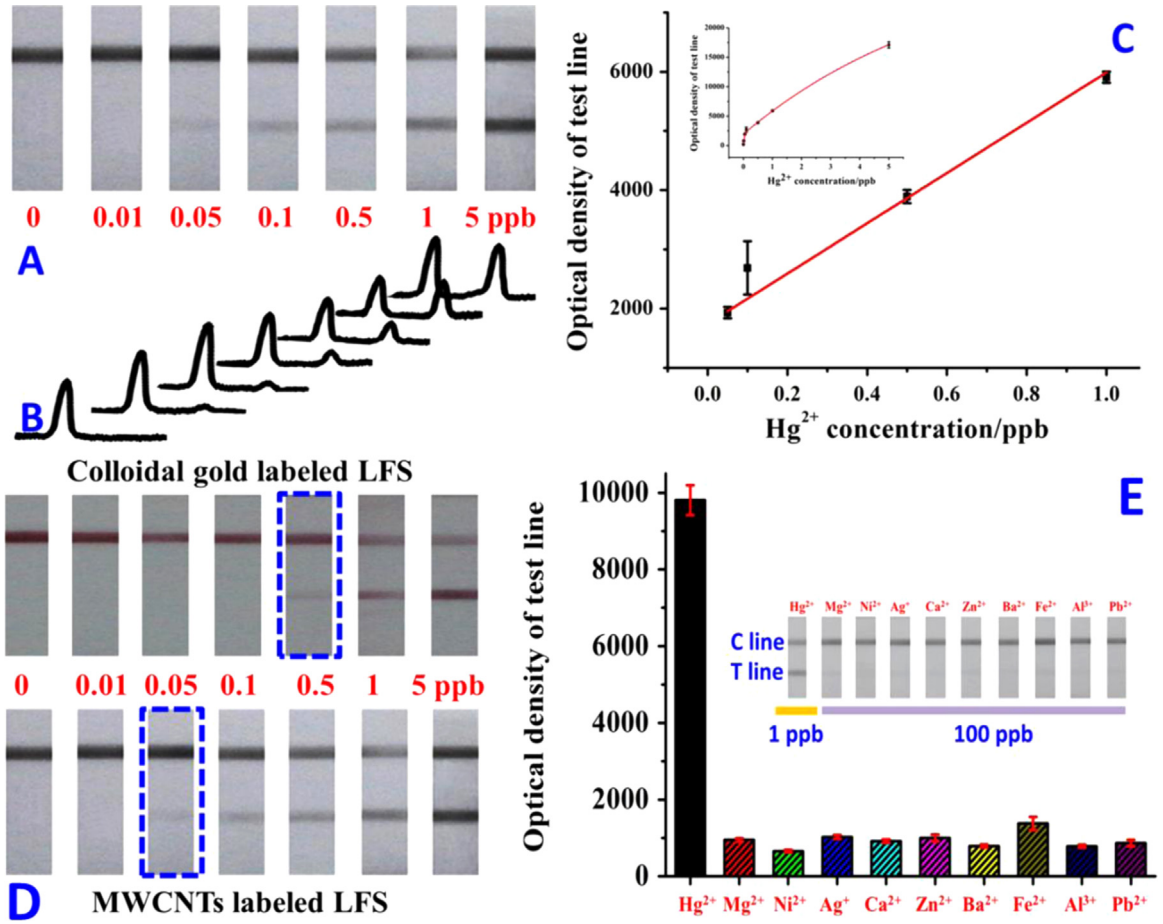

Fig. 3. (A) Hg^{2+} detection results image of MWCNT-LFS biosensor; (B) Quantitative Hg^{2+} detection results of the MWCNT-LFS biosensor by ImageJ; (C) Calibration curve of Hg^{2+} detections with MWCNT-LFS biosensor (the inset image: the variation rule in the whole detection concentration range); (D) Comparison results of Hg^{2+} detection between classic LFS and our MWCNT-LFS biosensor; (E) Specificity research results of the MWCNT-LFS biosensor (1 ppb of Hg^{2+}, 100 ppb of Mg^{2+}, Ni^{2+}, Ag^{+}, Ca^{2+}, Zn^{2+}, Ba^{2+}, Fe^{2+}, Al^{3+} and Pb^{2+}).

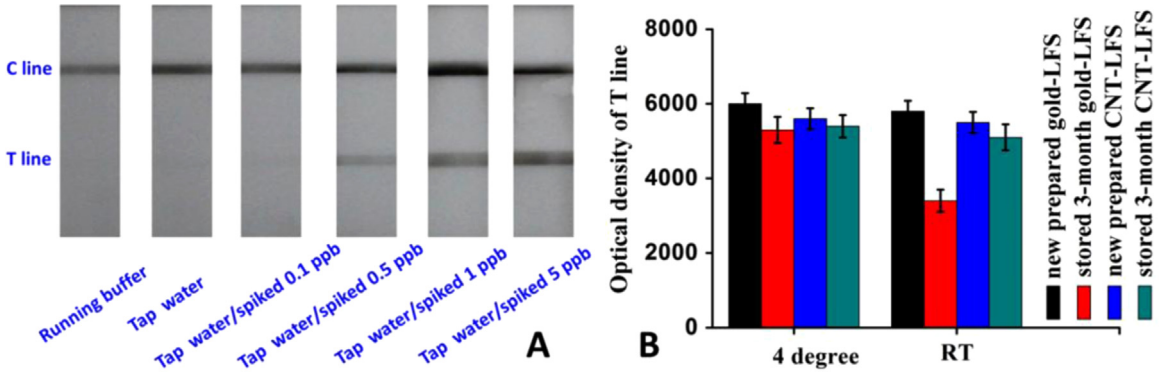

Fig. 4. (A) Detection results of real spiked tap water samples with MWCNT-LFS biosensor; (B) Stability comparison results of the classic LFS and MWCNT-LFS biosensor under different conditions.

Therefore, after functionalization the test probe with thiol, we assembled it on the surface of the colloidal gold with diameter of 25 nm by the stable covalent bond of Au-S. Also under optimal experimental conditions, we examined the performance of the gold nanoparticle-based test strip with different concentrations of target Hg^{2+}, to compare the detection sensitivity with the method using MWCNTs (Fig. 3(D)). From the results shown in Fig. 3(D), it can be concluded that the visual threshold of the MWCNT-based LFS biosensor was achieved at 0.05 ppb, while that of the traditional colloidal gold nanoparticle-based LFS was at 0.5 ppb. At least 10-fold improvement of the sensitivity of the LFS was achieved by using the MWCNTs as the labeling substrate instead of the traditional gold nanoparticles.

3.4. Specificity of the MWCNTs based LFS biosensor

To validate the specificity of this assay for Hg^{2+} detection, Mg^{2+}, Ni^{2+}, Ag^{+}, Ca^{2+}, Zn^{2+}, Ba^{2+}, Fe^{2+}, Al^{3+} and Pb^{2+} were used as controls. The detection results are demonstrated in Fig. 3 (E), in the presence of only 1 ppb of Hg^{2+}, the black band on the test zone can be observed clearly. However, even 100 ppb of other heavy metal ions (including Mg^{2+}, Ni^{2+}, Ag^{+}, Ca^{2+}, Zn^{2+}, Ba^{2+}, Fe^{2+}, Al^{3+} and Pb^{2+}) were loaded onto the LFS, no black signals were observed on the test lines and a black band can be observed only on the control lines indicating the effectiveness of the measurements. The corresponding statistic optical responses were further confirmed by recording the average optical density values of the black bands on the test zone (n=5). Altogether, there results indicated that this method can detect Hg^{2+} successfully without interference from other constituents, which could be ascribed to the excellent recognition specificity of the adopted nucleic acid probes.

3.5. Performance of MWCNT-LFS biosensor in complex sample matrix

Fig. 4 We further challenged the performance of the MWCNT-LFS biosensor with spiked Hg^{2+} in more complicated matrices, like tap water samples, tea water samples and lake water samples. When Hg^{2+} was spiked in the tap water and measured with the MWCNT-LFS biosensor directly, the test zone on the strip still showed a sensitive response to Hg^{2+} (Fig. 4(A)), and the tap water sample without Hg^{2+} was negative similar to that of the blank running buffer (Fig. 4(A)). The lowest detection limit of Hg^{2+} spiked tap water was about 0.5 ppb. Meanwhile, the detection results of the other two real spiked samples were in almost the same as that of the tap water samples (See results in supporting information). All these results confirm the feasibility of this approach for direct Hg^{2+} analysis in a complicated sample matrix.

Besides, as expected using MWCNTs for sensing performance improvement of LFS, another important factor of this research, the stability of the developed MWCNTs based strip biosensor, was also considered. The detection results of Hg^{2+} at 1 ppb with the new prepared and 3-month stored MWCNT-LFS biosensors at 4 °C and RT, respectively. Furthermore, the detection results of MWCNT-LFS biosensors were also compared to those of the colloidal gold based strip biosensors. After 3-month storage of the biosensors, the sensing optical density signal of traditional LFS biosensor decreased obviously compared to the new prepared ones. Of note, the sensing signal of MWCNT-LFS biosensor was almost not changed after long-term storage. All results shown in Fig. 4 (B) indicated that the stability of the MWCNT-labeled lateral flow strip was greatly improved compared with that of the colloidal gold-labeled ones even at RT. And this MWCNT-labeled LFS biosensor could be applied in wider fields under different detection conditions.

4. Conclusion

In summary, we have successfully constructed a novel strip biosensor using MWCNTs as color substrate for rapid and sensitive detection of Hg^{2+}. The mechanism of detection of Hg^{2+} is based on the covalent binding of amino with hydroxyl group for the assembly of MWCNT-DNA and the formation of T-Hg^{2+}-T sandwich structure, leading to the capture of MWCNTs on the test zone of the strip. With this biosensor, we can visually detect Hg^{2+} with 0.05 ppb in a standard sample within 15 min without instrumentation, which indicates more power for 10-fold lower detectable limit than the conventional colloidal gold based strip biosensor. In addition, the principle of the strip biosensor can be applied for detection in other types of samples such as the tap water, which also provides a satisfactory result. More importantly, the stability of the MWCNT-ssDNA conjugate and the assembled lateral flow strip greatly improves the sensing performance that could be further applied for the detection of other analytes.

Acknowledgements

This work is financially supported by the NSFC grant of 21475030, 31301460, the Science and Technology Research Project of Anhui Province 15czz03109, National 10000 Talents-Youth Top-notch Talent Program, the National and Zhejiang Public Benefit Research Project (201313010, 2014C32051) and the Jiangsu Science and Technology Support Program of BE201373, 2012780.

Appendix A. Supplementary material

Supplementary data associated with this article can be found in the online version at http://dx.doi.org/10.1016/j.bios.2016.05.031.

References

Abdolmohammad-Zadeh, H., Rahimpour, E.A., 2015. Sens. Actuators B Chem. 225, 258–266.
Andruch, V., Kocurova, L., Balogh, I.S., Skrlíkova, J., 2012. Microchem. J. 102, 1–10.
Anjaneyulu, Y., Rao, R.V.S., 2001. Can. J. Chem. Eng. 79 (1), 71–79.
Burstein, E., 2003. J. Fraklin. Inst. 340 (3–4), 221–242.
Chai, X., Chang, X., Hu, Z., He, Q., Tu, Z., Li, Z., 2010. Talanta 82 (5), 1791–1796.
Chen, Y., Yao, L., Deng, Y., Pan, D., Ogabiela, E., Cao, J., Adeloju, S.B., Chen, W., 2015. Microchim. Acta 182 (13–14), 2147–2154.
Deng, Y., Wang, X., Xue, F., Zheng, L., Liu, J., Yan, F., Xia, F., Chen, W., 2015. Anal. Chim. Acta 868, 45–52.
Dhamecha, D., Jalalpure, S., Jadhav, K., 2016. J. Photochem. Photobiol. B 154, 108–117.
Du, R., Zhao, Q., Zhang, N., Zhang, J., 2015. Small 11 (27), 3263–3289.
Ge, X., Zhang, W., Lin, Y., Du, D., 2013. Biosens. Bioelectron. 50, 486–491.
Giovanni, B., Gema, D.L.T., Guldi, D.M., Tomas, T., 2010. Chem. Rev. 110 (11), 6768–6816.
Gojny, F.H., Nastalczyk, J., Roslaniec, Z., Schulte, K., 2003. Chem. Phys. Lett. 370 (5–6), 820–824.
Guo, Z., Duan, J., Yang, F., Li, M., Hao, T., Wang, S., Wei, D., 2012. Talanta 93, 49–54.
Han, D., Lim, S.Y., Kim, B.J., Piao, L., Chung, T.D., 2010. Chem. Commun. 46 (30), 5587–5589.
He, P., Li, S., Dai, L., 2005. Synthetic Met. 154 (1–3), 17–20.
Hezard, T., Laffont, L., Gros, P., Behra, P., Evrard, D., 2013. Angew. Chem. Int. Ed. 119 (23), 4448–4451.
Kalluri, J.R., Arbneshi, T., Afrin Khan, S., Neely, A., Candice, P., Varisli, B., Washington, M., McAfee, S., Robinson, B., Banerjee, S., Singh, A.K., Senapati, D., Ray, P.C., 2009. Angew. Chem. Int. Ed. 121 (51), 9848–9851.
Li, D., Wieckowska, A., Willner, I., 2008. Angew. Chem. Int. Ed. 47, 3927–3931.
Li, S.D., Yu, Z., Rutherglen, C., Burke, P.J., 2004. Nano Lett. 4 (10), 2003–2007.
Li, S.N., He, P.G., Dong, J.H., Guo, Z.X., Dai, L.M., 2005. J. Am. Chem. Soc. 127 (1), 14–15.
Li, X., Li, W., Yang, Q., Gong, X., Guo, W., Dong, C., Liu, J., Xuan, L., Chang, J., 2014. ACS Appl. Mater. Int. 6 (9), 6406–6414.
Liao, Y., Wang, N., Ni, Y., Xu, J., Shao, S., 2015. J. Electroanal. Chem. 754, 94–99.
Liu, D., Huang, Y., Chen, M., Wang, S., Liu, K., Lai, W., 2015a. Food Control 50, 659–662.
Liu, G., Luo, Q., Wang, H., Zhuang, W., Wang, Y., 2015b. RSC Adv. 5 (86), 70109–70116.
Liu, J., Lu, Y., 2007. Angew. Chem. Int. Ed. 46, 7587–7590.
Lou, X., Detrembleur, C., Sciannamea, V., Pagnoulle, C., Jérôme, R., 2004. Polymer 45 (18), 6097–6102.
Luo, J.T., Wen, H.C., Wu, W.-F., Chou, C.P., 2008. Polym. Compos. 29 (12), 1285–1290.
Mao, X., Wang, W., Du, T.E., 2013. Talanta 114, 248–253.
Martínez, M.T., Tseng, Y.C., González, M., Bokor, J., 2012. J. Phys. Chem. C 116 (42), 22579–22586.
Mei, Z.L., Qu, W., Deng, Y., Chu, H.Q., Cao, J.X., Xue, F., Zheng, L., El-Nezamic, H.S., Wu, Y.C., Chen, W., 2013. Biosens. Bioelectron. 49, 457–461.
Mei, Z.L., Deng, Y., Chu, H.Q., Xue, F., Zhong, Y.H., Wu, J.J., Yang, H., Wang, Z.C., Zheng, L., Chen, W., 2012. Microchim. Acta 180 (3–4), 279–285.
Panchakarla, L.S., Govindaraj, A., 2008. J. Chem. Sci. 120 (6), 607–611.
Pirlot, C., Mekhalif, Z., Fonseca, A., Nagy, B., Demortier, J., Delhalle, G., 2003. J. Chem. Phys. Lett. 372 (3–4), 595–602.
Ramanathan, T., Fisher, F.T., Ruoff, R.S., Brinson, L.C., 2005. Chem. Mater. 17 (6).
Sanchez-Valencia, J.R., Dienel, T., Groning, O., Shorubalko, I., Mueller, A., Jansen, M., Amsharov, K., Ruffieux, P., Fasel, R., 2014. Nature 512 (7512), 61–64.
Senapati, T., Senapati, D., Singh, A.K., Fan, Z., Kanchanapally, R., Ray, P.C., 2011. Chem. Commun. 47 (37), 10326–10328.
Storelli, M., 2008. Food Chem. Toxicol. 46 (8), 2782–2788.
Tanaka, K., Clever, G.H., Takezawa, Y., Yamada, Y., Kaul, C., Shionoya, M., Carell, T., 2006. Nat. Nanotechnol. 1 (3), 190–194.
Wang, L.B., Chen, W., Ma, W.W., Liu, L.Q., Ma, W., Zhao, Y., Zhu, Y.Y., Xu, L.G., Kuang, H., Xu, C.L., 2011. Biosens. Bioelectron. 47, 1574–1576.
Wang, M., Yan, F.Y., Zou, Y., Yang, N., Chen, L., Chen, L.G., 2014a. Spectrochim. Acta A 123, 216–223.
Wang, Y.Z., Chen, S., Wei, C., Xu, M.M., Yao, J.L., Li, Y., et al., 2014b. Chem. Commun. 50 (65), 9112–9114.
Wang, Z., Li, H., Li, C., Yu, Q., Shen, J., De Saeger, S., 2014c. J. Agr. Food Chem. 62 (27), 6294–6298.
Wu, B., Hu, D., Kuang, Y., Liu, B., Zhang, X., Chen, J., 2009. Angew. Chem. Int. Ed. 48 (26), 4751–4754.
Xiao, S.J., Hu, P.P., Xiao, G.F., Wang, Y., Liu, Y., Huang, C.Z., 2012. J. Phys. Chem. B 116 (32), 9565–9569.
Zhang, S., Luo, H., Zhang, Y., Li, X., Liu, J., Xu, Q., Wang, Z., 2016a. Microchem. J. 126, 25–31.
Zhang, Z., Fu, X., Li, K., Liu, R., Peng, D., He, L., Wang, M., Zhang, H., Zhou, L., 2016b. Sens. Actuators B- Chem. 225, 453–462.
Zhou, J., Zhu, K., Xu, F., Wang, W., Jiang, H., Wang, Z., Ding, S., 2014. J. Agr. Food Chem. 62 (49), 12061–12066.
Zhu, M.Y., Wang, Y., Deng, Y., Yao, L., Samuel, B.A., Pan, D.D., Xue, F., Wu, Y.C., Zheng, L., Chen, W., 2014. Biosens. Bioelectron. 61, 14–20.